Thermochimica Acta, 117 (1987) 331–363
Elsevier Science Publishers B.V., Amsterdam – Printed in The Netherlands

Review

THE THERMAL DECOMPOSITION OF OXALATES. A REVIEW

D. DOLLIMORE

Department of Chemistry, University of Toledo, Toledo, OH 43606 (U.S.A.)

(Received 11 November 1986)

ABSTRACT

The thermal decomposition and stability of oxalates are reviewed from the viewpoint of their characteristic features rather than by a complete coverage of the existing literature, which is found to often be repetitive in nature.

INTRODUCTION

A review of oxalates seems pertinent under the present circumstances because the author has been working in this field for a long time [1], because they have industrial uses, many analytical applications [2] and because in many ways their thermal stability and decomposition serve as examples for the decompositions of many other oxysalts. It is possible to review the characteristic features of oxalate decompositions under various headings related to their behavior rather than by citing a complete list of publications. This is not meant to slight publications not mentioned but to allow the characteristic features to be highlighted. The presence of the oxalate ion

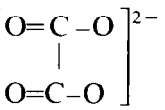

characterizes and identifies the compounds under review. The parent acid is oxalic acid, $(COOH)_2$. The salts of the simple oxalates show the oxalate ion combined with a single metal ion or with more than one [2]. There are usually various hydrated forms [2]. There are also more complex oxalates where other organic radicals can be incorporated into the structure. These, however, are not the subject of the present review. In the early publications the interaction of the oxalates upon decomposition with the atmosphere was neglected whilst as a generalization it may be said that many recent publications do not pay enough attention to the morphological form of the material. The crystal shape, size, the presence of defects and various prehistory treatments play an important part in the decomposition, especially in determining the kinetics of oxalate decomposition [3].

0040-6031/87/$03.50

DECOMPOSITION ROUTES FOR SIMPLE OXALATES

The decomposition routes for oxalates are affected by the environment—a fact not always appreciated by earlier workers.

Sketching out the primary decomposition routes for zinc oxalate demonstrates this point [4,5].

One has for zinc oxalate dihydrate the following sequence of decomposition reactions:

$$ZnC_2O_4 \cdot 2H_2O = ZnC_2O_4 + 2H_2O \quad (1)$$

Differential thermal analysis (DTA), peak endothermic in both N_2 and air,

$$ZnC_2O_4 = ZnO + CO + CO_2 \quad (2)$$

DTA peak, endothermic in N_2 in air or oxygen, however,

$$CO + \tfrac{1}{2}O_2 = CO_2 \quad (3)$$

The above reaction is catalyzed by the zinc oxide product surface and is exothermic. The exothermic nature of the catalyzed oxidation of carbon monoxide to carbon dioxide produces an overall exothermic character to the DTA peak for the decomposition of zinc oxalate in air or oxygen. The more

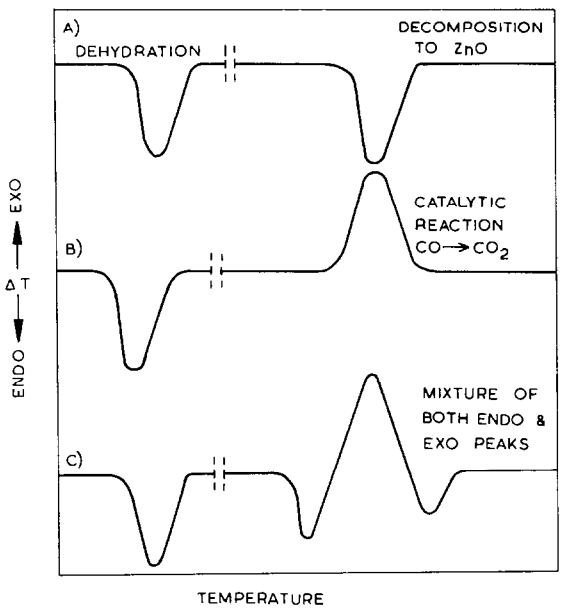

Fig. 1. DTA curves for zinc oxalate dihydrate in various atmospheres (schematic and not to scale): (A) in nitrogen, (B) in oxygen or air, (C) in oxygen or air where DTA pattern is more complex.

complicated DTA peaks observed sometimes for this part of the decomposition are due to the slow build up of solid zinc oxide which might not at first present enough surface to act as an effective catalyst. In the latter part of the reaction the sintering of the zinc oxide can reduce its catalytic efficiency. This produces the more complicated DTA signals found in some circumstances for this type of decomposition [6]. This is shown schematically in Fig. 1.

Nickel oxalate dihydrate follows quite different primary decomposition routes. A similar change, however, from an endothermic decomposition peak in nitrogen to an exothermic peak in air or oxygen is observed, but the reasons are different. The dehydration process is again endothermic in both nitrogen or air [7].

$$NiC_2O_4 \cdot 2H_2O = NiC_2O_4 + 2H_2O \tag{4}$$

DTA peak, endothermic in both N_2 and air.
The decomposition is to the metal:

$$NiC_2O_4 = Ni + 2CO_2 \tag{5}$$

DTA peak endothermic in N_2
In air, however, the metal is oxidized:

$$Ni + \tfrac{1}{2}O_2 = NiO \tag{6}$$

This is a violently exothermic reaction, especially at the temperature of decomposition. The pyrophoric nature of the metal is mainly due to its finely divided state giving it a specific surface area (from low temperature N_2 adsorption of around 150 $m^2\ g^{-1}$). The overall reaction in air is thus exothermic. Again, more complicated DTA signals may be found which arise because product nickel is initially present only in small quantities, and towards the end of the reaction the heat generated causes the metal to sinter and so become less pyrophoric, thus allowing the basic endothermic peak to reappear.

In addition, for nickel oxalate on decomposition in air, the product gas, CO_2, may shield the solid residue and not allow the oxygen to react with nickel metal until it is swept clear of the solid residue by the current of air or oxygen used in the DTA experiment. These points are schematically represented in Fig. 2.

It should be noted that dehydration is always endothermic and, where a carbonate is formed, then its decomposition is also endothermic under all environments. Thus, calcium oxalate monohydrate breaks down thermally as follows:

$$CaC_2O_4 \cdot H_2O = CaC_2O_4 + H_2O \tag{7}$$

DTA peak endothermic

$$CaC_2O_4 = CaCO_3 + CO \tag{8}$$

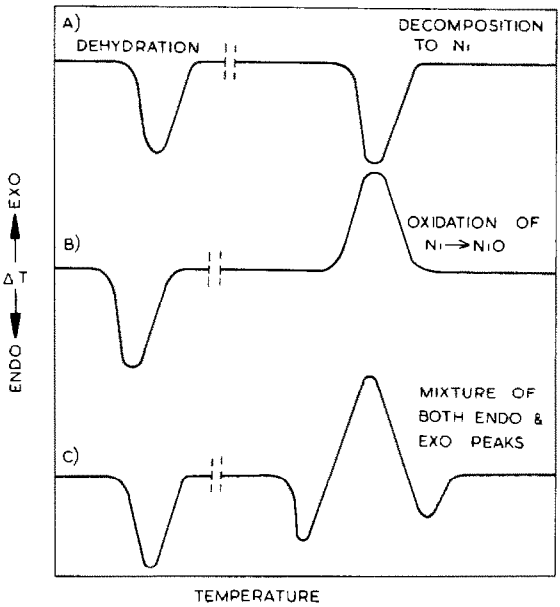

Fig. 2. DTA curves for nickel oxalate dihydrate in various atmospheres (schematic and not to scale): (A) in nitrogen, (B) in oxygen or air, (C) in oxygen or air where DTA pattern is more complex.

DTA peak, endothermic in N_2, often exothermic in air or O_2 and then

$$CaCO_3 = CaO + CO_2 \tag{9}$$

DTA peak endothermic.

The catalytic reaction

$$CO + \tfrac{1}{2}O_2 = CO_2 \tag{10}$$

is sometimes found to occur, being affected by parts of the DTA cell assembly which may act as catalysts.

In other variable valence oxalate decompositions, the reaction in nitrogen leads to the formation of the lowest valency oxide. In air or oxygen the oxide stable at the temperature of decomposition should be formed. This makes the decomposition route particularly dependent on the environment and in a later section the specific case of the thermal decomposition of manganese oxalate is cited [8,9].

The occurrence of carbon in the solid product residues is persistently reported particularly for the rare earth oxalates [10,11]. Thus for lanthanium oxalate at least some of the exothermic peaks observed in a DTA run in air or oxygen atmosphere are due to oxidation of carbon which is one of the products of the oxalate decomposition [12].

Praseodymium oxalate hydrate is an example where carbon may be found in the product solid residues. The main decomposition route can be written:

$$Pr_2(C_2O_4)_3 \cdot 10H_2O \rightarrow Pr_2(C_2O_4)_3 \rightarrow Pr_2O(CO_3)_2 \rightarrow Pr_2O_2CO_3 \quad (11)$$

yielding Pr_7O_{12} in a helium/oxygen mixture, Pr_2O_3 in helium and in carbon dioxide. All DTA peaks were endothermic in He and CO_2, but exothermic peaks appear in helium/oxygen mixtures.

In an inert atmosphere carbon was noticed in the solid product. In carbon dioxide an endothermic peak could be attributed to

$$C + CO_2 \rightarrow 2CO \quad (12)$$

The exothermic peaks in helium/oxygen mixtures can be assigned to;

$$\begin{aligned} C + O_2 &\rightarrow CO_2 \\ CO + \tfrac{1}{2}O_2 &\rightarrow CO_2 \end{aligned} \quad (13)$$

TABLE 1

Primary decomposition products of simple oxalates [a]

Oxalate	Product
Cobalt	Metal
Nickel	
Cadium	
Tin	
Lead	
Antimony	Antimony and bismuth give a mixture
Bismuth	of metal and oxide
Silver	
Magnesium	Oxide
Aluminum	
Chromium(III)	
Manganese(II)	
Iron(III)	
Zinc	
Iron(II)	In iron(II) oxalate the metal is also formed depending on conditions
	Oxide and some carbon
Cerium(III)	
Thorium(IV)	
Praseodymium	
Lanthanum	
Lithium	Carbonate
Sodium	
Potassium	
Calcium	
Strontium	
Barium	

[a] This list is by no means complete and for reservations as to its applicability see the remarks in the text.

and

$$2CO \rightarrow C + CO_2 \quad (14)$$

The formation of carbon is attributed to the direct decomposition of $Pr_2O(CO_3)_2$ to the oxide and carbon dioxide [10]. This is not necessarily a main stoichiometric reaction but possibly only a side reaction. Thorium oxalate also decomposes to an oxide plus a carbon [13].

Copper oxalate [4], mercuric oxalate [14] and silver oxalate [15,16] all decompose in nitrogen with an exothermic reaction. These decompositions are often described as auto-catalytic.

Ammonium oxalate decomposes endothermically and in a similar manner both in nitrogen and oxygen. The decomposition remains endothermic in oxygen because there is no solid product, all decomposition products are gaseous, and there is no catalyst surface to act as a catalyst for oxidation reactions [4]. Table 1 is produced here with some reservations showing the probable primary product with the decomposition of some simple oxalates. The reservations are that local conditions imposed upon the experiment and material and even the pre-history of the material itself could cause different reaction routes to appear [4,5].

MECHANISM

Attempts were made by Kornienko [17] and by Robin [18] to relate decomposition temperatures with the fundamental properties of the metal ions for transition/metal oxalates. Robin plotted the onset temperature of decomposition against the atomic number for oxalates of manganese, ferrous iron, cobalt, nickel and zinc. The result is a continuous curve with a minimum, with Fe^{3+} and Cu^{2+} as exceptions (see Fig. 3).

The decomposition temperature of the copper oxalate does not fit into the general pattern. It is also difficult from such a plot to understand why materials such as the oxalates of chromium, manganese, iron and zinc, which produce oxides as a result of decomposition both in air and in nitrogen, should be expected to fit any scheme including cobalt, nickel and copper oxalate which give the oxide on decomposition in air but the metal in nitrogen.

In oxalates (A)

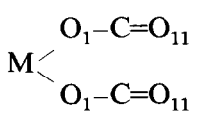

of bivalent metals, the extent to which the metal–O_1 bond is covalent depends on the electronegativity of the metal. Decomposition will occur when a temperature is reached at which rupture of the M–O link is possible,

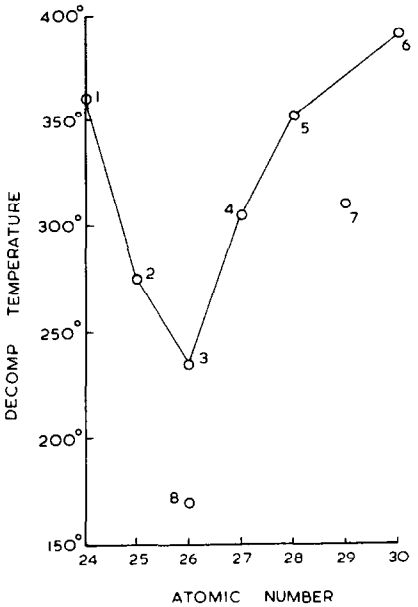

Fig. 3. Plot of the decomposition temperature of simple oxalates in air against atomic number [18]: (1) Cr^{3+}, (2) Mn^{2+}, (3) Fe^{2+}, (4) Co^{2+}, (5) Ni^{2+}, (6) Zn^{2+}, (7) Cu^{2+}, (8) Fe^{3+}.

or at which rupture of the $C-O_1$ bond occurs. Fujita et al. [19] suggested from infrared studies that as the $M-O_1$ bond becomes stronger, so the $C-O_1$ bond is lengthened and the $C-O_1$ bond is shortened.

If the reaction proceeds by rupture of the $C-O_1$ bond, this would be followed by rupture of the second M–O bond, because of the inability of the metal to accommodate two oxygen atoms. The total reaction would lead to the evolution of equimolecular proportions of carbon monoxide and carbon dioxide. An alternative possibility, which has been shown to take place in the decomposition of silver oxalate, is the direct rupture of the two M–O bonds to produce the metal with the liberation of carbon dioxide [16].

For those oxalates which produce the metal in nitrogen the decomposition temperature represents the temperature at which the M–O link is ruptured and will depend critically on the size and charge of the metal ion, whereas in those decompositions where the oxide is produced in nitrogen the decomposition temperature represents the energy required to break the $C-O_1$ bond and this will depend less critically on the nature of the cation.

In those decompositions which proceed to the metal, the decomposition temperature should be related to the lattice energy, which is given by:

$$E_0 = \frac{e^2 X}{r_i} \tag{15}$$

where E_0 is the lattice energy, X is a constant, e is the charge on the ions

and r_i is their separation. When $e = 2$, then

$$T_D = \frac{\text{Constant}}{(r_m + r_{ox})} \tag{16}$$

where T_D, the absolute decomposition temperature, is taken as being proportional to E_0 (the log of maximum rate is assumed to be the same for each decomposition), and r_m and r_{ox} are the radii of the metal and the oxalate ion, respectively.

Thus, for bivalent metals,

$$\frac{1}{T_D} = \frac{r_m}{\text{Constant}} + \frac{r_{ox}}{\text{Constant}} \tag{17}$$

This relationship was tested by Dollimore et al. [5] by plotting $1/T_D$ against r_m for bivalent transition metal oxalates. A linear plot was obtained for all these oxalates which decomposed to the metal as predicted by the model, whilst manganese and zinc oxalates lie off the line so produced. It is these two oxalates which produce an oxide as the primary solid product. The relationship has since been tested in other oxysalt systems but in view of the fact that equipment has been improved, that the data is dependent on the instrument design, and that values of crystal ionic radii are not always agreed this relationship really needs a careful reexamination [20].

However, these kind of arguments really ignore the ionic structure of most of these oxalates with the metal ion and the oxalate ion existing as separate entities in the solid lattice. Boldyrev et al. [21] suggest that all three decomposition schemes,

$$M_2C_2O_4 \rightarrow \begin{cases} MCO_3 + CO \\ MO + CO \cdot\cdot CO_2 \\ M + 2CO_2 \end{cases} \tag{18}$$

originate from breakdown of the oxalate anion due to bond rupture,

$$C_2O_4^{2-} \rightleftharpoons 2CO_2^- \tag{19}$$

This intermediate is converted to the carbonate (due to carbonyl–carbonate intermediate) or to CO_2 (by electron transfer):

$$CO_2^- \rightarrow [OCOCO_2]^{2-} \rightarrow CO_3^{2-} + CO \rightarrow O^{2-} + CO_2 + CO \tag{20}$$

or

$$CO_2^- \rightarrow CO_2 + 2e^- \tag{21}$$

and

$$M^{2+} + 2e^- \rightarrow M \tag{22}$$

THERMODYNAMIC CONSIDERATIONS

If one studies the reaction types involved in the dehydration and decomposition of oxalates they are of two types:

$$A_{(s)} \rightarrow B_{(s)} + G_{(g)} \tag{23}$$

where the important factor is the liberation of a single gaseous species.

Examples are

$$CaC_2O_4 \cdot H_2O_{(s)} \rightarrow CaC_2O_{4(s)} + H_2O_{(g)} \tag{24}$$

$$NiC_2O_4 \rightarrow Ni + 2CO_2 \tag{25}$$

and

$$CaCO_3 \rightarrow CaO + CO_2 \tag{26}$$

The second type of decomposition is of the type:

$$A_{(s)} \rightarrow B_{(s)} + G_{(g)} + F_{(g)} \tag{27}$$

where two gaseous species are evolved. An example of this second type is:

$$ZnC_2O_4 \rightarrow ZnO + CO + CO_2 \tag{28}$$

One gaseous species liberated

For the first type of dissociation, where only one gaseous species is involved, then the variation of the equilibrium or dissociation pressure with temperature can be shown by conventional thermodynamic methods [6]. The approximate equation

$$\frac{\mathrm{d} \ln P}{\mathrm{d}T} = \frac{\Delta H}{RT^2} \tag{29}$$

expresses the dependence of the equilibrium pressure of X(g) on the temperature, where R is the gas constant and ΔH is the ordinary heat of reaction at the temperature T (in Kelvin). This is of identical form to that which applies to phase equilibrium. The true equilibrium constant K_f is equal to the fugacity (f) of the gas in equilibrium with the solid at a total pressure of 1 atm (the standard state). Strictly, it is the variations of $\ln f$ with the temperature which is given by:

$$\frac{\mathrm{d} \ln f}{\mathrm{d}T} = \frac{\Delta H^\circ}{RT^2} \tag{30}$$

where ΔH° is the heat of reaction adjusted to a low value of the total pressure when the gases behave ideally. Experimentally, however, it is the partial pressure p which is measured (equivalent K_p^1) and in most cases no attempt is made to keep the total pressure at 1 atmosphere. The matter is discussed in greater detail in another study [22].

Integration of the simple expression gives:

$$\ln K_p = -\frac{\Delta H}{RT} + \text{const.} \tag{31}$$

or

$$\ln P_{P_g} = -\frac{\Delta H}{RT} + \text{const.} \tag{32}$$

Over a small temperature range the dependence of the decomposition upon the environmental pressure is now obvious. Many systems conform to these expectations even if not strictly irreversible in the thermodynamic sense. Thus, if product gas is present in the gas phase above the decomposing oxalate then the decomposition temperature corresponds to the temperature obtained by substituting appropriate values of P_{P_g} in the above equation. The DTA experiments are most useful for this kind of measurement when the variation of the peak temperature or the onset temperature with pressure can be used to construct plots of log (pressure) against $1/T$. This has been done for dehydration dissociation [23,24], for carbonate dissociation [25] and for oxide dissociation [26]. It does not seem to have been utilized systematically in the case of oxalate systems.

Two gaseous species liberated

The general equation gives either eqn. (31) or

$$\ln P_{P_{G(g)}} P_{P_{G(g)}} = -\frac{\Delta H}{RT} + \text{const.} \tag{33}$$

It should be possible to hold one of these partial pressures constant and show the variation of partial pressure with decomposition temperature using DTA techniques. Again, this has not been attempted, although it seems a feasible experiment.

The arguments can be developed, however, to predict which reaction will predominate for the two possible routes:

$$MC_2O_4 \rightleftharpoons MO + CO + CO_2 \tag{34}$$

and

$$MC_2O_4 \rightleftharpoons M + 2CO_2 \tag{35}$$

This has been done by Dollimore et al. [5,27]. The Ellingham free energy diagrams showing the variation of the free energy of formation with temperature [27] are utilized for this purpose and the relevant information is schematically portrayed in Fig. 4.

If the discussion is confined to equilibrium conditions, then for reaction (34), the equilibrium constant (K) is given by:

$$K_1 = \frac{[MO][CO][CO_2]}{[MC_2O_4]} \tag{36}$$

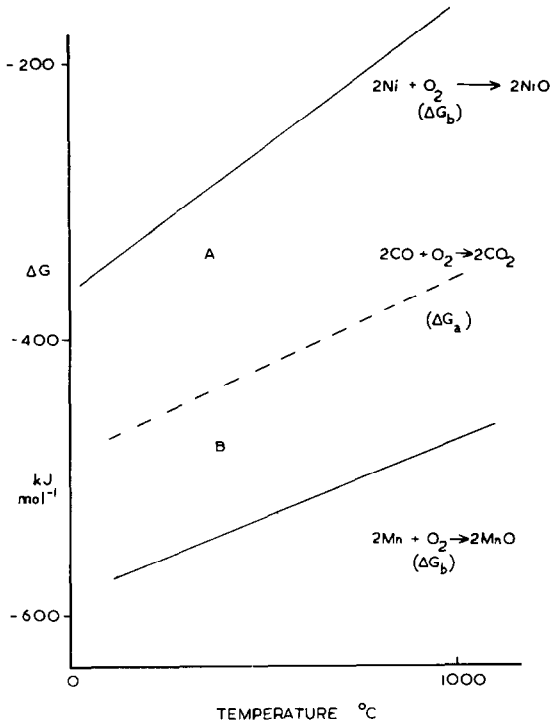

Fig. 4. Variation in the free energy of formation (ΔG) of various oxides with temperature schematically displayed [27].

and for reaction (35), the equilibrium constant (K_2) is given by

$$K_2 = \frac{[M][CO_2]^2}{[MC_2O_4]} \tag{37}$$

In both instances the square brackets denote activities. Then,

$$\frac{K_1}{K_2} = \frac{[MO][CO]}{[M][CO_2]} \tag{38}$$

A similar ratio can be obtained from a consideration of the reactions

$$2CO + O_2 = 2CO_2 \tag{39}$$

and

$$2M + O_2 = 2MO \tag{40}$$

i.e.

$$\left(\frac{K_4}{K_3}\right)^{1/2} = \frac{[MO][CO]}{[M][CO_2]} \tag{40a}$$

where K_3 is the equilibrium constant for reaction (39) and K_4 that for reaction (40). It follows that

$$\frac{K_1}{K_2} = \left(\frac{K_4}{K_3}\right)^{1/2} \tag{41}$$

If the standard free energy of formation ($\Delta G^\circ = -RT \ln K$) for reaction (39) is denoted by ΔG_a and for reaction (40) by ΔG_b, then for $\Delta G_a > G_b$ there must exist the relationship

$$K_3 < K_4 \tag{42}$$

and from eqn. (41) it follows that

$$K_1 > K_2 \tag{43}$$

Therefore, if reactions (34) and (35) are considered at equilibrium, reaction (34) is more to the product side than is reaction (35); or, alternatively, reaction (34) will predominate over reaction (35).

The variation of the free energy of formation of the various oxides under consideration are provided in graphical form by Ellingham and shown schematically in Fig. 4. In this diagram the various values of ΔG_b for several systems are given by the full lines whilst the values of ΔG_a are represented by the dotted line. To make this clearer in the figure only two typical lines for ΔG_b are provided, one above and one below the ΔG_a line. In Ellinghams original diagrams a large number of systems were portrayed.

When the ΔG_b line is below the ΔG_a line, as it is for zinc, manganese and tin, then under equilibrium conditions reaction (34) predominates over reaction (35) and when the ΔG_b line is above the ΔG_a line, as it is for copper, lead, nickel, cobalt and cadmium, then the reverse is true. Ferrous iron is unique in that the ΔG_b line crosses the ΔG_a line at a temperature above 700 °C and lies only just above it at the decomposition temperature.

In this case Broadbent et al. were later able to demonstrate that the residues of this decomposition contained free iron, Fe_3O_4 and FeO [28].

Similar arguments can be set out for the oxalates of trivalent metal ions for which three reactions are possible. Of these two are analogous to the decomposition schemes for the divalent metal oxalate, with a third to yield the trivalent oxide M_2O_3. These are

$$M_2(C_2O_4)_3 = 2MO + 4CO_2 + 2CO \tag{44}$$

$$M_2(C_2O_4)_3 = 2M + 6CO_2 \tag{45}$$

and

$$M_2(C_2O_4)_3 = M_2O_3 + 3CO_2 + 3CO \tag{46}$$

If reactions (44) and (45) are set up as equilibria, reaction (44) is more to the product side than is reaction (45), if ΔG_a exceeds ΔG_b. Similarly, for reactions (44) and (46), the condition $\Delta G_a > \Delta G_c$ (where ΔG_c is the free

energy change for the reaction $4MO + O_2 = 2M_2O_3$) must be observed if reaction (46) is to be set up more to the product side than reaction (44). For reaction (44) to be set up under equilibrium conditions more to the product side then reaction (45) the condition is that $\Delta G_a > \Delta G_d$ (where ΔG_d is the free energy charge for the reaction $\frac{4}{3}M + O_2 = \frac{2}{3}M_2O_3$).

All these arguments apply to equilibrium conditions; removal of gaseous products as they are formed, e.g. in a stream of nitrogen, would favour the tendency shown by most systems to produce only one final solid product, i.e. the metal or the oxide, rather than mixture. Where the thermodynamic argument suggests that a metal should predominate in the solid residue from the reaction in nitrogen (e.g. the oxalates of copper, nickel, cobalt and cadmium): in oxygen, of course the oxide is produced. These observations are well exemplified by nickel oxalate which in nitrogen yields two endothermic peaks, the second representing decomposition to the metal. In air or oxygen the second peak becomes exothermic due to oxidation of the metal (see Fig. 3).

EFFECT OF ENVIRONMENT

It has already been pointed out that the course of oxalate decomposition may be affected by the environment. Ignorance of this led early workers in the field to claim that oxalate decompositions were exothermic in character, whereas it is now quite clear that the majority of such decompositions in an inert atmosphere are endothermic [29,30].

The most obvious change caused by the environment is when the actual product is different due to the influence of the surrounding gas atmosphere. This point has already been made with regard to the primary decomposition routes followed by the decomposing oxalate. The decomposition of manganese oxalate to yield a series of different oxide products depending on experimental conditions is an example that may be cited [8,31]. The product in vacuum, nitrogen or any other inert gas is the green oxide, MnO, whilst the product in oxygen is one of the other manganese oxides, MnO_2, Mn_2O_3 or Mn_3O_4, recognized by their black or brownish-black color, the exact nature of this product depending on "local" conditions adjacent to the decomposing sample, the container design and the packing and amount of sample used in the experiment. In order of increasing temperature the transformation temperature for these oxides at one atmosphere of air has been given by Honda and Stone [32] as:

$$MnO_2 \xrightarrow{535\,^\circ C} Mn_2O_3 \xrightarrow{933\,^\circ C} Mn_3O_4 \xrightarrow{1160\,^\circ C} MnO \qquad (47)$$

The accuracy of these early observations may be in doubt, especially that for $Mn_3O_4 \rightarrow MnO$ conversion, and because some of these oxides occur in

several forms. It would seem that a general rule is the oxide stable at the temperature of decomposition in air or at a particular pressure of oxygen is the product oxide ultimately formed in the thermal decomposition of manganese oxalate [33].

There is another environmental effect, namely the shape and size of the container crucible and the material with which it was constructed. Thus the endothermic or exothermic character of the decomposition of magnesium oxalate can be affected in this manner. The decarboxylation peak in air is endothermic except in the presence of a catalyst [34]. If a platinum crucible is used this can provide the appropriate catalyst surface and the reaction becomes exothermic overall.

Simons and Newkirk showed clearly that factors affecting decomposition are sample size, heating rate, the atmosphere and container geometry [35], and this has been confirmed many times on a variety of systems and samples. In particular the variation of mass of sample has a profound affect on the rate determining step in kinetic determinations [36,37].

KINETIC CONSIDERATIONS

Most solid state decompositions are governed by the movement of a reaction interface which determines the kinetics. There are other factors which have been discussed fully elsewhere [38–43].

The shape of the original particles largely determines the subsequent changing shape of the reaction interface and hence the kinetics. If the reaction rate per unit area of interface is constant then a zero order reaction will result. This would result with growth of reaction interface from the two large faces of platelet crystals. In its simplest forms the single crystal behavior is inferred from the shape, as seen in the kinetics for spherically-shaped reaction interfaces contracting inwards or the contracting area conditions also observed in certain cases. These models will produce deceleratory kinetic laws. It is often assumed that such simplistic models reflect the behavior of single particles multiplied by a factor which represents the total weight of the sample. However, in powder compacts an additional factor is the spread of the reaction interface via the points of adhesion [44]. Galwey [45] has detailed many of the factors governing the kinetics and mechanism of thermal decomposition of transition metal carboxylates.

Oxalates have been the subject of attempts to elucidate kinetics by rising temperature techniques and calcium oxalate has figured in such studies under the claim that it can be considered a model material [46,47]. The problem is however that rising temperature techniques largely obscure many aspects of solid state kinetics, such as the occurrence of an induction period [48], and the observation of the anomalous effect of water vapor known as the Smith–Topley effect [49]. This latter effect is known to occur on the

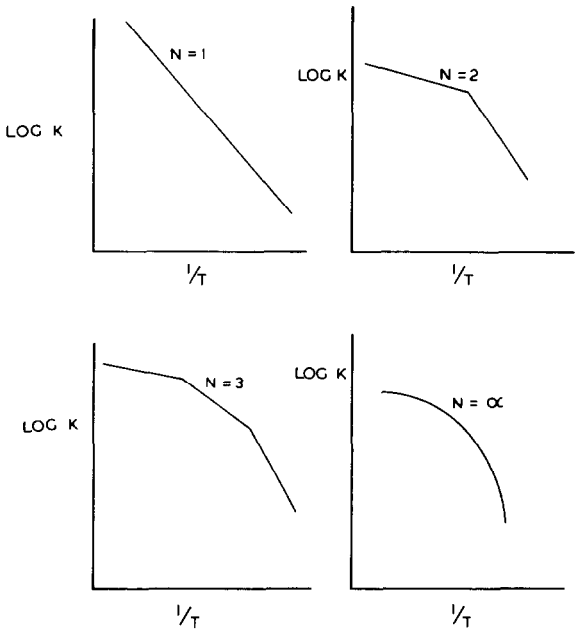

Fig. 5. Different plots of log k against $1/T$ demonstrating typical deviations from "normal behavior".

dehydration of calcium and magnesium oxalates [50–53]. Furthermore the rising temperature methods if thoughtlessly applied hide effects due to the pre-history of the sample. Thus, the kinetics of cobalt oxalate have been shown by isothermal kinetic studies to be greatly influenced by the prior conditions of dehydration [48]. Attempts to place the sample actually in a mass spectrometer and follow the kinetics have been successful technically, but the environmental aspect of an oxalate decomposition in this special set of surroundings makes the application of the findings to more general kinetic studies open to speculation, although the data collected in this way is of a very basic nature [47]. Furthermore, the many attempts to produce a kinetic analysis from rising temperature methods using the integral approach are most often based on the assumption that a single Arrhenius plot describes the kinetic behavior [38]. The comments of Koch [54] on the chemical compensation effect and in particular that the use of E and A permit a more selective characterization of a reaction then solely one of these values or the rate constant at 298 K are important. There is in fact a spread of E values but A values tend to be found within a defined range. It is important to establish the Arrhenius plot and its behavior, as in many cases deviations have been reported (see Fig. 5). The commonest deviations shown by many oxalate decompositions are demonstrated in this figure, namely a set of n separate linear Arrhenius plots. The values of n range from $n = 1$ to $n = \alpha$; $n = 1$ corresponds to the norm, and $n = \alpha$ corresponds

to a curved plot of log K again $1/T$. The accuracy of the data collected is normally such that beyond $n = 4$, it is impossible to attach a value for n and to all intents n appears as infinity and a curve is observed. From this it is seen that a rising temperature kinetic evaluation on an oxalate decomposition must establish not only the value of A and E but the n sets of A and E necessary to establish a complete description of the kinetic process. Most integral methods of establishing E are based on the assumption that $n = 1$ and are thus suspect. However, the simple derivative approach to establish rising temperature kinetics puts the Arrhenius expression to the test and the values of n and the various sets of A and E can be readily established.

PHASE TRANSITIONS

Phase changes intrude upon the decomposition sequence in a number of cases associated with the solid products of oxalate decomposition. If phase changes occur on the DTA heating curve which are endothermic then the phase change occurring is the conversion of a phase stable over a definite temperature range to another phase stable at higher temperatures. An example is the phase change occurring in barium carbonate. This type of endothermic transition is reversible and on a DTA plot obtained during the cooling cycle appears as an exothermic effect. Dell and Wheeler [55] claim to observe an exotherm transition from an amorphous to a crystalline phase during the decomposition of certain oxalates on the heating program of the

TABLE 2

Decomposition data on barium oxalate ($BaC_2O_4 \cdot \frac{1}{2}H_2O$) heated for half an hour at indicated temperature in air [56] [a]

Temperature (°C)	Weight loss (%)	Density of solid residue (g cm^{-3})	Comment
100	0	1.866	Specific surface area 0.5 m^2 g^{-1}
210	4.0	1.92	Dehydration
308	4.3	2.06	
402	4.4	2.15	Specific surface 3.1 m^2 g^{-1}
460	12.0	2.70	Specific surface area 8.4 m^2 g^{-1}
495	15.6	3.74	Decomposition to γ-$BaCO_3$
556	15.9	4.18	
655	16.0	4.89	Specific surface area 9.7 m^2 g^{-1}
745	16.1	4.52	
800	16.1	4.40	
860	16.1	4.54	Due to transition to β-$BaCO_3$
900	16.1	4.39	

[a] Samples weighing 0.5 g used in each experiment.

TABLE 3

Summary of phase changes in oxalate decompositions on DTA [4]

Material	Character of peak	Departure from base line (°C)	Peak temperature (°C)
Potassium oxalate	Endo	370	388
Barium carbonate	Endo	795	802
Calcium carbonate [a]	Exo	643	653
Strontium carbonate	Endo	920	925
Cobalt oxide	Endo	955	968
Manganese oxide	Endo	1004	1011
Lead oxide	Endo	780	797
		850	857

[a] Only shown in 20% diluted samples.

DTA but their data is open to alternative interpretations. An exothermic phase change on the heating program of a DTA experiment can in general have several implications but in all cases represents an "energy rich" system changing to a stable system and is irreversible and so is not reflected on the cooling curve. It may indicate a low-temperature form which is metastable with respect to a higher temperature form or it may represent an "amorphous" form changing to a crystalline phase. The exothermic recrystallization process may sometimes be observed by decomposing the oxalate in vacuo and then admitting air: after an induction period, recrystallization occurs with the liberation of heat. In this case there is a dependence on the environmental atmosphere. (This must not be confused with the violent exothermic oxidation of a metal product under these conditions, e.g. nickel oxalate decomposing in nitrogen.)

It is not always necessary to use DTA to identify phase changes. Simple measurements such as the determination of density often suffice [56]. Thus, in the case of barium oxalate mentioned earlier this data could be used to show the existence of the β form of $BaCO_3$ (see Table 2). The sudden small but noticeable alteration in the density of the solid residue at around 850 °C is due to the transition from γ-$BaCO_3$ to β-$BaCO_3$ [56]. Table 3 indicates some of the phase changes observed in the thermal decomposition of oxalates [4].

TEXTURAL CHANGES

The physical texture of the solid residues can be affected by the environment. To investigate such changes can entail the use of optical or electron microscopy and work on zinc oxalate may be quoted as examples of such studies [57–60]. Physical textural changes are more likely to affect the

kinetics of the thermal decomposition rather than the main decomposition route [45]. The use of gas adsorption studies based on the physical adsorption of nitrogen is a method which has often been used to follow the changes in texture during decomposition [1]. The determination of density can also be used to follow the physical state of the solid residue left after thermal decomposition [56,61] and this has been applied to cobalt oxalate decomposition [62].

The factors which matter are the shape and size of the original reacting particles, the degree of compaction and adhesion between particles imposed on the material under investigation, and whether the product gases are removed as quickly as possible under vacuum conditions or at atmospheric under specified conditions of flow.

Theoretical principles governing the changes in particle size or surface area during the course of decomposition were clearly outlined by Gregg [63]. Quantitative correlations can be made between the kinetics of decomposition and the surface area [64], and have been applied to the decomposition

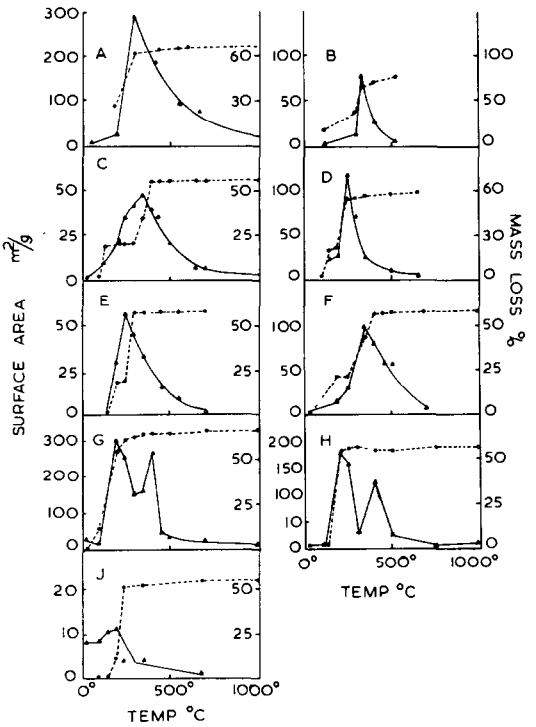

Fig. 6. The variation of the specific surface area of residues from oxalate decomposition against the temperature of heat treatment with the mass loss also shown [1]: dotted line, mass loss; full line, surface area. (A) Aluminum oxalate, (B) chromium(III) oxalate, (C) zinc oxalate, (D) manganese(II) oxalate, (E) cobalt(II) oxalate, (F) nickel(II) oxalate, (G) iron(III) oxalate, (H) iron(II) oxalate, (J) copper(II) oxalate.

of lithium oxalate by Dollimore and Tinsley [65]. Generally there is on heating an oxalate such as zinc oxalate an initial increase in surface area which is eventually overtaken by the sintering process [1]. Typical plots of this kind are shown in Fig. 6. The increase in surface area or the decrease in particle size is caused by a shattering of the particles. This is caused by strains set up due to differences in the densities of the solid reactant and product causing a distortion of the reaction interface. The process of disruption leading to a maximum surface area does not necessarily coincide with the completion of chemical decomposition. It would, however, be expected to be accompanied by a heat change [66]. The fact that this does not appear on DTA curves is probably due to the magnitude of the heat change involved. However, a variation in particle size or surface texture of the original particles might be expected to cause a change in the base line of the DTA trace where the sample was originally packed in a manner that ensures maximum thermal conduction. An alteration in this packing by the above disruptive processes could well be reflected in base-line drift. The density changes noted earlier can be used with the corresponding surface areas to make a quantitative estimate of the disruption caused by the heat treatment [1,61]. The relationship between these two quantities can be expressed as:

$$\frac{V_1}{V_2} = \left(\frac{S_1}{S_2}\right)^{\frac{3}{2}} N^{\frac{1}{2}} \tag{47}$$

where V_1 is the molar volume of the starting material (the oxalate) and S_1 the molar surface area. The density determinations allow V_1 to be calculated. The subscript 2 refers to the same quantities for the equivalent amount of solid product. N is the number of particles formed from a single reactant particle and is thus a measure of the strain set up within the system.

THE DEHYDRATION STEP

At first, the dehydration step in the thermal treatment of oxalates seems straightforward in that it is always endothermic in character. It is left this late in the review to discuss this initial stage in decomposition because it is affected by a combination of factors which include a consideration of the kinetics and the texture of the solid residue. The DTA trace can often reveal separate stages to the dehydration not shown by the TG.

Thus the dehydration process in vacuum or low water vapor pressure often produces an amorphous anhydrous material with a high surface area whilst at a higher vapor pressure of water a crystalline anhydrous product results with a much smaller surface area. This has been observed for the dehydration of certain oxalates and other oxysalts. It is called the

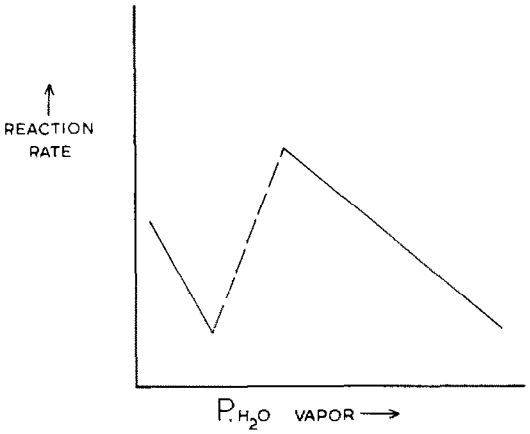

Fig. 7. Schematic representation of the Smith–Topley effect—the anomalous variaton of the dehydration rate with the environmental pressure of water vapor above the sample.

Smith–Topley effect [49,67]. It has been observed for the dehydration of manganese oxalate dihydrate [49], calcium oxalate monohydrate [50,51,52,68] and magnesium oxalate dihydrate [53]. A schematic representation of the Smith–Topley effect is shown in Fig. 7. This shows that at low pressures of water vapor the dehydration rate constant decreases with increasing water vapor pressure until a critical pressure is reached. The rate constant then increases sharply and in the higher pressure region the behavior in the presence of water vapor becomes normal. The initial behavior upon dehydration at low relative vapor pressure of the water vapor has been shown to be associated with the production of an amorphous dehydrated product whilst in the second region at higher water vapor crystalline. One can represent the low pressure system as

$$MC_2O_4 \cdot xH_2O_{(s)} = MC_2O_{4\text{amorphous}} + xH_2O_{(v)} \tag{48}$$

which behaves normally with respect to water vapor pressure. Here $MC_2O_4 \cdot xH_2O_{(s)}$ represents the solid hydrated oxalate, $MC_2O_{4\text{amorphous}}$ the amorphous dehydrated product.

At high vapor pressures a second system operates which again behaves normally with respect to water vapor pressure and this can be represented as

$$MC_2O_4 \cdot xH_2O_{(s)} = MC_2O_{4\text{crystalline}} + xH_2O \tag{49}$$

where $MC_2O_{4\text{crystalline}}$ represents the crystalline dehydrated product. Thus the abnormal behavior is simply the appearance of the amorphous product under vacuum or low water vapor conditions and the appearance of a crystalline product in the higher vapor pressure region. It would also seem necessary to explain why the effect is not widely reported for other vapors or gases.

A very simple explanation of the Smith–Topley effect is to note that the strain caused at the reaction interface during decomposition is often sufficient to cause complete disruption of the solid residue with an increase in surface area so that the product appears amorphous to X-ray diffraction techniques [63]. However, above a certain low critical vapor pressure, water vapor has a profound effect upon ionic mobilities either through the surface or through the bulk of the solid. This is a well known phenomenon in sintering and has been demonstrated on zinc oxide prepared by the thermal treatment of zinc oxalate [69]. The effect is to cause a recrystallization process to occur or a growth in particle size so that the material becomes crystalline to X-ray diffraction studies. One therefore has beyond a given vapor pressure of water a crystalline anhydrous product appearing in contrast to the amorphous anhydrous product appearing in the vacuum or low water vapor region. Such an explanation explains the Smith–Topley effect very simply but Watelle–Marion et al. [68] have put forward alternative explanations based upon the appearance of a metastable phase established when the temperature and pressure imposed upon the initial system are far removed from the condition of equilibrium. If the metastable phase is considered to appear because of the strain set upon the system particularly at the reaction interface then the two explanations have a common basis.

In certain infrequent cases the water is retained until after decomposition of the oxalate. This is found mainly with basic and ill-defined oxalates such as basic aluminum oxalate. Occasionally a small amount of water (up to 2–3%) may be released at a temperature much higher than the main dehydration or decomposition stage. This probably represents water in the crystal structure of hydrates occluded in anhydrous crystals and liberated later because of physical changes (involving perhaps some change in density) in the micro-structure of the material. This permits diffusion of the water to the surface.

It will be observed that in determining the kinetics of dehydration with a rising temperature program that the Smith–Topley effect is not observed. This is to be expected as there is one extra parameter—the temperature being altered and gas is removed as fast as it is formed [70,71]. The reversibility of these hydration reactions has recently attracted attention [72].

USE OF VARIETY OF TECHNIQUES

The investigator should not expect the results from different techniques to exactly match. Each technique imposes special conditions upon the sample which may not be present in another technique. In thermal analysis the heating rate is important. The TG curves of most transition metal oxalates, for example, show no stable dehydration states when obtained at a fast

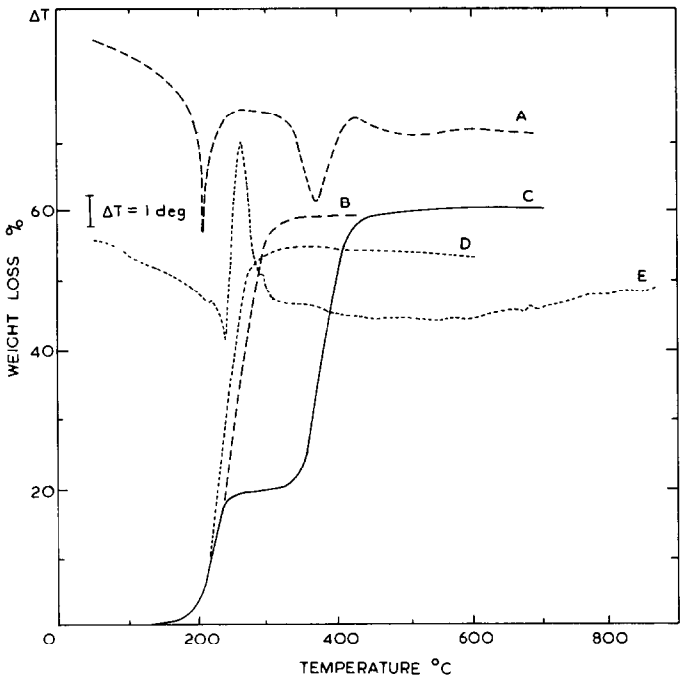

Fig. 8. (A, B) DTA curves for $FeC_2O_4 \cdot 2H_2O$ in nitrogen and air, respectively; (C, D, E) TG curves for $FeC_2O_4 \cdot 2H_2O$ in nitrogen at a fast heating rate, in nitrogen at a slow heating rate and in air in that order [28].

heating rate, whereas DTA curves distinguish separate stages. Thus, in most TG experiments on ferrous oxalate dehydrate in air, and in fast TG experiments in nitrogen, it is difficult to observe the anhydrous material as a separate stage, but in slow TG determinations in nitrogen the dehydration and decomposition steps can be separated (Fig. 8). The exact heating rates involved depend on the equipment, the amount of material, and rate at which gas is passed over the sample [5,28]. On the DTA curve in air (using much smaller masses of sample than for the TG experiments), the dehydration is largely overshadowed by the exothermic reaction associated with decomposition and oxidation. In nitrogen, however, the DTA curve shows the dehydration and decomposition as separate stages. The DTA signal is simply not being generated in an environment that will achieve the clearest and most accurate TG trace. In spite of this the use of combined and simultaneous TG and DTA can prove to be useful. It allows, for example, a very easy correlation of temperatures. This can be seen in experiments on the decomposition of the oxalates or uranium [73]. In nitrogen the decomposition of $UO_2C_2O_4$ to UO_2 appears as an exothermic reaction, whereas the decomposition of $U(C_2O_4)_2$ to UO_2 is endothermic. In air, both decompositions are exothermic, but that of $UO_2C_2O_4$ is enhanced and becomes a

two-peak system. The first part of the peak is due to decomposition of $UO_2C_2O_4$ to UO_2, whilst the second part is due to the oxidation of UO_2 to U_3O_8. Figure 9 shows all these results [73].

The effect of the experimental environment often caused by the technique itself can thus cause alterations in the course of the chemical reaction, and the texture of the solid residue. It is possible that these alterations may be reflected in the thermodynamic nature of the reaction, i.e. the position of the

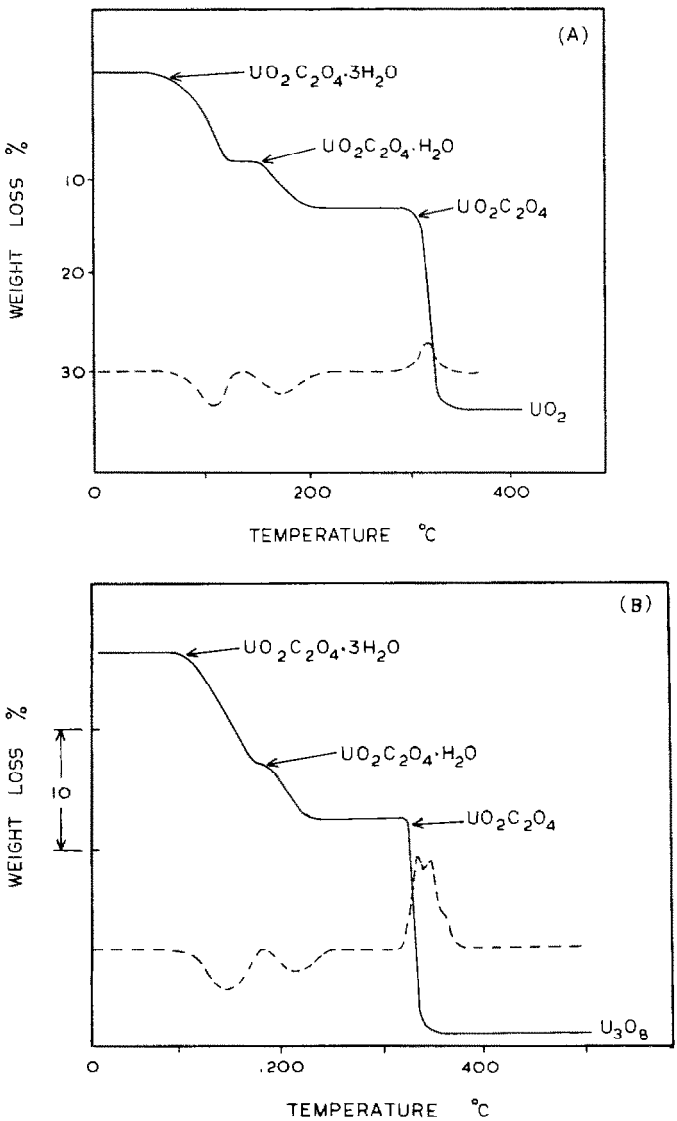

Fig. 9. Simultaneous TG and DTA curves for (A) $UO_2C_2O_4 \cdot 3H_2O$ in nitrogen, (B) $UO_2C_2O_4 \cdot 3H_2O$ in air, (C) $U(C_2O_4)_2 \cdot 6H_2O$ in nitrogen, (D) $U(C_2O_4)_2 \cdot 6H_2O$ in air [73].

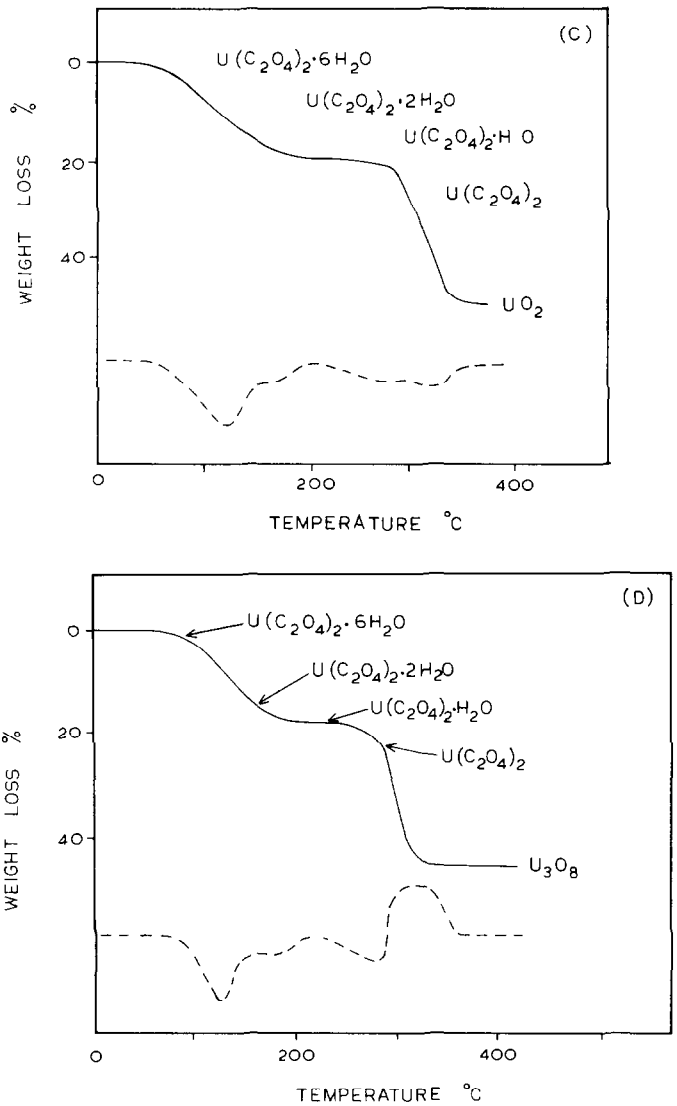

Fig. 9 (continued).

equilibrium state, or in the kinetics of the thermal decomposition. Other special techniques also impose special environments peculiar to the technique. Thus the direct study of dehydration in the electron microscope may pose difficulties as the electron beam itself can cause damage to texture or even dehydration. The use of the mass spectrometer for gas analysis when the sample is placed in the mass spectrometer can create a very special environment [47,74].

Infrared absorption spectroscopy has frequently been used to identify the initial oxalates or their decomposition products. Thus Jere and Patel studied

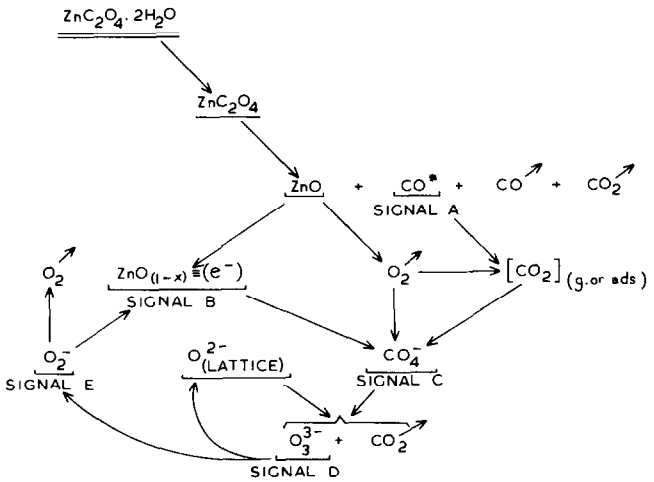

Fig. 10. Summary of the successive reactions identified by EPR occurring during the thermal decomposition of zinc oxalate dihydrate [76,77].

the thermal decomposition of proxy titanium oxalate, using a combination of infrared and DTA techniques [75]. Their infrared data led them to assign the structure of the starting material as:

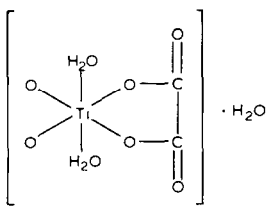

Electron paramagnetic resonance has been used extensively by Gabelica, Hubin and Derouane and associates [76,77] to compliment TG data and identify successive steps at the reaction interface in the vacuum decomposition of oxalates. A complicated sequence of reactions is demonstrated and Fig. 10 shows their summary of reactions for the vacuum decomposition of zinc oxalate dehydrate in vacuum.

COMPLEX OXALATES

In coordination compounds generally the thermal stability is often affected by the tendency of the external ion to enter the coordination sphere. Usually the oxalate ion tends to enter the coordination sphere. The tendency for many coordinating agents to occupy more than one coordinating position to form a ring often imparts thermal stability. Those chelate rings which

are generally most stable are rings containing five or six members including the metal ion. The oxalate anion $C_2O_4^{2-}$ in common with other polyvalent ions such as CO_3^{2-} can coordinate with a metal ion by chelation. The formula of the complex oxalato species is generally of the form, $M^I[M^{II}(C_2O_4)_n]^x$. The oxalato species can be represented by $MC_2O_4^+$, $MC_2O_4^-$, $M(C_2O_4)_2^-$, $M(C_2O_4)_2^{3-}$, $M(C_2O_4)_3^{2-}$, $M(C_2O_4)_3^{3-}$, $M(C_2O_4)_3^{2-}$, $M(C_2O_4)_4^{4-}$, and $M(C_2O_4)_4^{5-}$.

The valency of the metal species M in these formulae can readily be ascertained but sometimes takes the form MO^{2+} (i.e. TiO^{2+}, VO^{2+}), MO_2^{2+} (i.e. OsO_2^{2+}, UO_2^{2+}) or MO_3^+ (i.e. NbO_3^+, TaO_3^+).

The oxalate group can also take the form of a hydrogen oxalate group thus increasing the possible ways of attachment to the central metal species.

The infrared spectra of oxalato complexes helps to understand the nature of the bonds involved and hence their structure. There have been many such studies [19,78–88]. Douville et al. [79] explained their results in terms of the vibrations associated with the bonds in the structure:

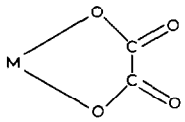

Deductions based on the 1 : 1 metal ligand model of the chelate ring of tri(oxalato) Cr(III) produced values for the metal–oxygen stretching bands at 600–300 cm^{-1} for various oxalato complexes [83]. The argument used for the simple oxalates applies here, namely that the frequencies of uncoordinated C=O stretching bands (υ, 1700–1600 cm^{-1}) increased and those of coordinated C–O stretch bands (υ, 1450–1350 cm^{-1} and 1300–1200 cm^{-1}) decreased as the frequency of the metal–oxygen (M–O) stretching band (υ, 600–500 cm^{-1}) increased.

There is a tendency in some oxalates for oxalic acid to appear as an adduct. This occurs to some slight extent with strontium but can be readily observed with barium [89–93]. There are a whole series of oxalate salts involving the barium cation.

Like the simple oxalates the DTA curves for complex oxalates often show a dependence with the nature of the environmental gas, showing an endothermic decomposition in nitrogen and an exothermic process in air [94]. Dehydration remains unaffected by the atmosphere and endothermic in character. The endothermic decomposition in nitrogen becomes exothermic in air due to catalytic conversion of carbon monoxide to carbon dioxide with the solid product providing the catalytic surface. The exothermic change upon decomposition of potassium oxalato complexes of cobalt(II) and nickel(II) in air from an endothermic decomposition in nitrogen is probably caused by oxidation of the metal produced in the primary decomposition reaction (Fig. 11).

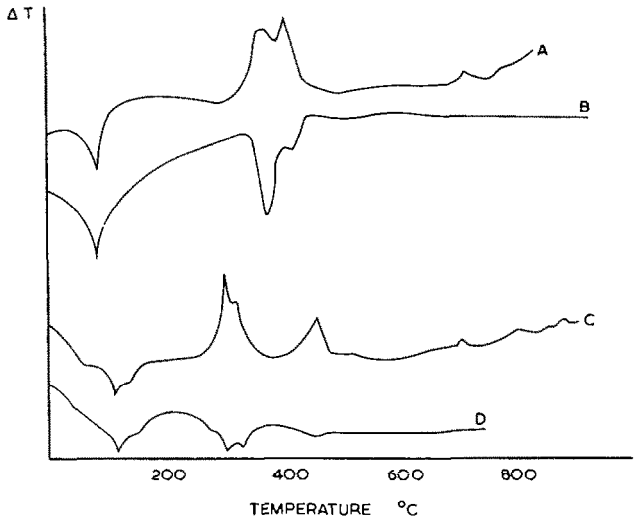

Fig. 11. DTA curves for (A) $K_3Al(C_2O_4)_3 \cdot 2H_2O$ in air, (B) $K_3Al(C_2O_4)_3 \cdot 2H_2O$ in nitrogen, (C) $K_2TiO(C_2O_4)_2 \cdot 2H_2O$ in air, (D) $K_2TiO(C_2O_4)_2 \cdot 2H_2O$ in nitrogen [94].

Valency changes occur in the decomposition sequence of some complex oxalates. Thus Gallagher and Kurkjian [95] showed valency changes in complex oxalates of iron(III) to iron(II) in the early stages of decomposition. They used Mossbauer spectra to demonstrate their findings. Broadbent et al. [28] were able to prepare anhydrous ferrous oxalate by decomposing ammonium iron(III) oxalate $(NH_4)_3Fe(C_2O_4)_3 \cdot 3H_2O$ in nitrogen at 200 °C.

The changes in the valency state of iron observed by Gallagher [96] during the thermal decomposition of barium and strontium iron(II) oxalato complexes are shown in Table 4. Subsequent oxidation of iron(II) in the oxide system involves an uptake of oxygen from the atmosphere.

In the series $K_3M(C_2O_4)_3 \cdot nH_2O$ (where M = Mn, Fe, Co, Cr, Al, V, Rh, Ga; $n = 3, 4, 5$) except for the chromium complex, all the complexes upon heating gave the anhydrous complex which then underwent dissociation to the corresponding oxide and potassium carbonate mixtures [28,97–101].

Based on studies involving the decomposition of $K_3[Fe(C_2O_4)_3]$ and $K_3[Co(C_2O_4)_3]$, Tanaka and Nanjo [102] suggest that there is electron transfer from the coordinated oxalate ion to the central metal ion. Negase's [103] statement that the thermal stability of the anhydrous complex decreases as the electron affinity of the central metal ion increases is in accord with Tanaka and Nanjo's suggestion. Expanding on this central theme and from experimental observation on the gas evolved during the thermal decomposition of complex oxalates Negase [104] found three types of decomposition. One group (oxalato complexes of Mn(III), Fe(III), Co(III), Rh(III), Cu(II), Pd(II) and Pt(II)) in an inert atmosphere gave only carbon dioxide as the gaseous product, produced by electron transfer from an

TABLE 4

The thermal decomposition of $Ba_3[Fe(C_2O_4)_3]_2 \cdot 8H_2O$ and $Sr_3[Fe(C_2O_4)_3]_2 \cdot 2H_2O$ in oxygen [96] [a]

Temperature range (°C)	Compound formed	Gases evolved
$Ba_3[Fe(C_2O_4)_3 \cdot 8H_2O$		
50–175	$Ba_3[Fe(C_2O_4)_3]_2$	$8\ H_2O$
175–300	$Ba_3Fe_2(C_2O_4)_5$	$2\ CO_2$
300–400	$3\ BaCO_3 \cdot Fe_2O_3$	$CO_2 + 6\ CO$
300–800	$BaCO_3 \cdot 2BaFeO_{2.8}$	$1.4\ CO_2 + 0.6\ CO$
750–900	$Ba_3Fe_2O_{6.6}$	CO_2
800	$Ba_3Fe_2O_6$	$0.3\ O_2$
$Sr_3[Fe(C_2O_4)_3]_2 \cdot 2H_2O$		
100–175	$Sr_3[Fe(C_2O_4)_3]_2$	$2\ H_2O$
175–350	$Sr_3Fe_2(C_2O_4)_5$	$2\ CO_2$
300–450	$3\ SrCO_3 \cdot Fe_2O_3$	$CO_2 + 6\ CO$
500–650	$SrCO_3 \cdot 2SrFeO_{2.8}$	$1.4\ CO_2 + 0.6\ CO$
700–900	$Sr_3Fe_2O_{6.6}$	CO_2
800	$Sr_3Fe_2O_6$	$0.3\ O_2$

[a] There is overlap in some stages cited.

oxalato ligand to a central metal ion. A second group gave one molecule of carbon dioxide for every molecule of carbon monoxide evolved (e.g. oxalato complexes of Al (III)), where decomposition occurred by C–O bond breaking to form a metal oxide with no change in the valence of the central metal. Finally there was a group where decomposition involved both the above processes, with the evolution of carbon dioxide and smaller amounts of carbon monoxide (e.g. complexes of V(III) and Cr(III)).

A further group was later studied by Negase et al. [105]. This group conformed to the general formula $K_2M(C_2O_4)_2$. The anhydrous oxalates of this general formula then either broke down to the metal oxide and potassium oxalate (M = Be(II), Mn(II) and Zn(II)) or to the metal and potassium oxalate (M = Co(II), Ni(II) and Cv(II)).

In the case of many of these systems a thermodynamic approach can help decide if mixed oxides with spinel structure will be formed. Mehandjiev et al. [106] put forward the following simple explanation which is really a consequence which can be inferred from the Ellingham free energy diagrams [27].

The thermodynamic probability has to be considered for the formation of either two single oxides:

$$A + 2B + \left(\frac{x}{2} + y\right)O_2 = AO_x + 2BO_y \tag{50}$$

or a mixed spinel oxide:

$$A + 2B + 2O_2 = AB_2O_4 \tag{51}$$

Under given conditions of temperature and oxygen pressure let the change in free energy be designated $\Delta G_{T(50)}$ for reaction (50) and $\Delta G_{T(51)}$ for reaction (51). The assumption has to be made that both are thermodynamically possible, i.e.

$$\Delta G_{T(50)} < 0 \tag{52}$$

and

$$\Delta G_{T(51)} < 0 \tag{53}$$

The reaction (51) leading to spinel formation will occur predominantly if

$$\Delta G_{T(51)} < \Delta G_{T(50)} \tag{54}$$

If

$$\Delta G_{T(50)} < \Delta G_{T(51)} \tag{55}$$

then a mixture of single oxides is formed, AO_x and BO_y being the thermodynamically most stable oxide under these conditions.

The formation of a mixed oxide with spinel structure can be represented as the sum of two consecutive processes;

$$A + 2B + 2O_2 = AO + B_2O_3 \tag{56}$$

The Gibbs free energy for this can be designated as $\Delta G_{T(56)}$.

The second process then gives the spinel structure,

$$AO + B_2O_3 = AB_2O_4 \tag{57}$$

The Gibbs free energy for this process can be designated as $\Delta G_{T(57)}$. It also follows that

$$\Delta G_{T(51)} = \Delta G_{T(56)} + \Delta G_{T(57)} \tag{58}$$

From eqns. (54) and (58) it follows that for spinel formation

$$\Delta G_{T(57)} < \Delta G_{T(50)} - \Delta G_{T(56)} \tag{59}$$

The minimal free energy of spinel formation, $\Delta G_{T(57)}$, from simple oxides will be obtained if the most favorable process for the single metal–oxygen systems, A–O and B–O, considered separately, are the formation of the monoxide AO and the sesquoxide B_2O_3 such that

$$\Delta G_{T(50)} = \Delta G_{T(56)} \tag{60}$$

Stated more generally, mixed spinel oxides may be obtained with the greatest probability in those temperature and oxygen ranges where both AO and B_2O_3 are thermodynamically stable oxides. Table 5 lists the temperature ranges for various oxides and spinels where there is the greatest region of thermodynamic stability. On the basis that a system of separate oxides or a

TABLE 5

Stability of oxide systems based on Gibbs free energy values at 0.21 atm pressure of oxygen [106]

Oxide	Stability region (K)
Regions of stability for oxides B_2O_3	
Fe_2O_3	< 450–1500
Cr_2O_3	625– > 2500
Mn_2O_3	750–1400
Co_2O_3	< 450–500
Regions of stability for oxides AO	
NiO	750– > 2500
CoO	1125– > 2500
MnO	1815– > 2500
CuO	< 450–1300
Regions of stability for spinels AB_2O_4	
$MnCo_2O_4$	500–1800
$NiCo_2O_4$	500–750
$CuCo_2O_4$	< 450–500
$FeMn_2O_4$	1500–1850
$NiMn_2O_4$	800–1375
$CoMn_2O_4$	1125–1400
$CuMn_2O_4$	700–1350
$NiFe_2O_4$	785–1500
$CoFe_2O_4$	1160–1510
$CuFe_2O_4$	< 450–1315
$MnFe_2O_4$	1500–1845
$NiCr_2O_4$	750– > 2500
$CoCr_2O_4$	1160– > 2500
$MnCr_2O_4$	1845– > 2500
$CuCr_2O_4$	625–1315

spinel is formed according to these predictions the end products of the decomposition of complex oxalates can be predicted.

REFERENCES

1 D. Dollimore and D. Nicholson, J. Chem. Soc., (1962) 960.
2 K.V. Krishnamurthy and G.M. Harris, Chem. Rev., 61 (1961) 213.
3 M.E. Brown, D. Dollimore and A.K. Galwey, in C.H. Bamford and C.F.H. Tipper (Eds.), Comprehensive Chemical Kinetics, Vol. 22, Elsevier, Amsterdam, 1980, p. 218.
4 D. Dollimore and D.L. Griffiths, J. Therm. Anal., 2 (1970) 229.
5 D. Dollimore, D.L. Griffiths and D. Nicholson, J. Chem. Soc., (1963) 2617.
6 D. Dollimore, J. Therm. Anal., 11 (1977) 185.
7 D. Broadbent, D. Dollimore and J. Dollimore, J. Chem. Soc. A, (1966) 278.

8 M. Brown, D. Dollimore and A.K. Galway, J. Chem. Soc., Faraday Trans. 1, 70 (1974) 1316.
9 D. Dollimore and N.M. Guindy, Thermochim. Acta, 58 (1982) 191.
10 Y. Saito and S. Sasaki, Netsusoketei, 7 (1980) 67.
11 P.K. Gallagher and F. Schrey, Thermochim. Acta, 1 (1970) 465.
12 R. Mobius, Wiss. Z. Tech. Hochsch. Chem. Leuna-Merseburg, 6 (1964) 359.
13 O.K. Srivastava and A.R. Vasudeva Murthy, J. Sci. Ind. Res. India, 21B (1962) 525.
14 Y.A. Ugai, Zh. Obsh. Khim., 24 (1954) 1315.
15 R.M. Haynes and D.A. Young, Discuss. Faraday Soc., 31 (1961) 229.
16 J.Y. MacDonald and C.N. Hinshelwood, J. Chem. Soc., 127 (1925) 2764.
17 V.P. Kornienko, Ukrain. Khim. Zh., 23 (1957) 159.
18 J. Robin, Bull. Soc. Chim. Fr., (1953) 1078.
19 J. Fujita, K. Nakamoto and M. Kaboyashi, J. Phys. Chem., 61 (1957) 1014.
20 D. Dollimore, N.J. Manning and D.V. Nowell, Thermochim. Acta, 19 (1977) 37.
21 V.V. Boldyrev, I.S. Nev'yantsev, Y.I. Mikhailov and E.F. Khairetdinov, Kinet. Katal., 11 (1970) 367.
22 D. Dollimore, J. Therm. Anal., 13 (1978), 455.
23 P. Barret and R. Thiard, C.R. Acad. Sci., Ser. C, 260 (1965), 2823.
24 L.G. Berg, I.S. Rassonskaya and E.V. Buris, Izv. Sekt. Fiz-khim. Anal. Inst. Obsh., 27 (1956) 239.
25 H. Henmi, T. Hirayama, N. Mizutani and M. Kato, Thermochim. Acta, 96 (1985) 1945.
26 T. Matsushima and W.J. Thoburn, Can. J. Chem., 43 (1965) 602.
27 D. Dollimore and G.R. Heal, Lab. Pract., 30 (1981) 221.
28 D. Broadbent, D. Dollimore and J. Dollimore, J. Chem. Soc. A, (1967) 451.
29 D.A. Young, Decomposition of Solids, Pergamon Press, New York, 1966, Chapt. 5, p. 148.
30 W.E. Garner, Chemistry of Solid State, Butterworths, London, 1955, p. 232.
31 D. Dollimore, J. Dollimore and J. Little, J. Chem. Soc., (1969) 2946.
32 K. Honda and T. Stone, Sci. Rept. Tohoka Imp. Univ., 3 (1914) 139.
33 D. Dollimore and K.H. Tonge, Proceedings of the Fifth International Symposium on Reactivity of Solids, Munich, (1964) 97.
34 D. Dollimore and J. Mason, Thermochim. Acta, 43 (1981) 183.
35 E.L. Simons and A.E. Newkirk, Talanta, 11 (1964) 549.
36 K. Krishnan, K.N. Ninan and P.M. Madhusudanan, Thermochim. Acta, 89 (1985) 295.
37 K.N. Ninana, Thermochim. Acta, 74 (1984) 143.
38 M.E. Brown, D. Dollimore and A.K. Galwey, in C.H. Bamford and C.F.H. Tipper (Eds.), Comprehensive Chemical Kinetics, Vol. 22, Elsevier, Amsterdam, 1980, p. 41.
39 J. Šesták, Thermophysical Properties of Solids, Vol. XII, Part D of G. Svehla (Ed.), Comprehensive Analytical Chemistry, Elsevier, Amsterdam, 1984, Chapt. 8, p. 172.
40 B. Delmon, Introduction à la Cinétique Heterogène, Technip, Paris, 1969.
41 P. Barret, Cinétique Heterogène, Gauthier-Villars, Paris, 1973.
42 D. Dollimore, National Bureau of Standards, Special Publication 580, Proceedings of Workshop on State of the Art of Thermal Analysis, Gaithersburg, MD, 1980, p. 1.
43 D. Dollimore, G.R. Heal and R.W. Krupay, Thermochim. Acta, 24 (1978) 293.
44 W. Komatso, in G.M. Schwab, Reactivity of Solids, Proc. 5th Int. Symp., Elsevier, Amsterdam, 1965, p. 182.
45 A.K. Galwey, Kinet. Katal., (English Trans.), 10 (1969) 626.
46 A.M.M. Gadalla, Thermochim. Acta, 74 (1984) 255.
47 D. Price, D. Dollimore, N.S. Fatemi and R. Whitehead, Thermochim. Acta, 42 (1980) 323.
48 D. Broadbent, D. Dollimore and J. Dollimore, J. Chem. Soc. A (1966) 1491.
49 M.L. Smith and B. Topley, J. Chem. Soc., (1935) 321.

50 L. Walter-Levy and J. Laniepce, C.R. Acad. Sci., Ser. C, 259 (1964) 4685.
51 M. Norbert Gerard and G. Watelle-Marion, C.R. Acad. Sci., Ser. C, 261 (1965) 2363.
52 D. Dollimore, T.E. Jones and P. Spooner, J. Chem. Soc. A (1970) 2809.
53 D. Dollimore, G.R. Heal and J. Mason, Thermochim. Acta, 24 (1978) 307.
54 E. Koch, Non Isothermal Reaction Analysis, Academic Press, London, 1977, p. 58.
55 R.M. Dell and V.J. Wheeler, 5th Int. Symp. Reactivity of Solids, Munich, 1964, p. 395.
56 D. Dollimore and D.V. Nowell, in I. Buzas (Ed.), Thermal Analysis, Proc. 4th ICTA, Academiai Kiado, Budapest, 3 (1975), p. 63.
57 R. Giovanoli, H.R. Oswald and W. Feitknecht, J. Microsc. (Paris), 4 (1965) 711.
58 R. Giovanoli, J. Microsc. (Paris), 6 (1967) 261.
59 R. Giovanoli and H.G. Widemann, Helv. Chim. Acta, 51 (1968) 1134.
60 G. Djega-Mariadassov, G. Pannetier and R. Giovanoli, J. Microsc. (Paris), 15 (1972) 323.
61 D. Dollimore and J. Pearce, J. Therm. Anal., 6 (1974) 321.
62 N. Armstrong, P. Campion, J.L. Dawson, D. Dollimore and C.E. Wood, J. Chem. Soc., (1963) 2556.
63 S.J. Gregg, J. Chem. Soc., (1953) 3940.
64 D. Nicholson, Trans. Faraday Soc., 61 (1965) 990.
65 D. Dollimore and D.M. Tinsley, J. Chem. Soc. A, (1971) 3043.
66 D. Dollimore, in R.C. MacKenzie (Ed.), Differential Thermal Analysis, Vol. 1, Academic Press, London, 1970, Chapt. 13, p. 395.
67 M.L. Smith and B. Topley, Proc. R. Soc., London, Ser. A, 134 (1931) 244.
68 R. Hocart, G. Watelle-Marion, A. Thrierr-Sorel and N. Gerard, C.R. Acad. Sci., Ser. C, 260 (1965) 2509.
69 D. Dollimore and P. Spooner, Trans. Faraday Soc., 67 (1971) 2750.
70 S. Gurrieri, G. Siracusa and R. Cali, J. Therm. Anal., 6 (1974) 293.
71 Y. Masuda, Y. Ho, R. Ho and K. Iwata, Thermochim. Acta, 99 (1986) 205.
72 M. Bark, B. Channaa, M. Lallemant and G. Bertrand, Thermochim. Acta, 97 (1986) 369.
73 R. Bressat, B. Caludel and Y. Trambouze, Bull. Soc. Chim. Fr., (1963) 464.
74 P.K. Gallagher, Thermochim. Acta, 26 (1978) 175.
75 G.V. Jere and C.C. Patel, Indian J. Chem., 2 (1964) 383.
76 E.G. Derouane, Z. Gabelica, R. Hubin and M.J. Hubin-Franskin, Thermochim. Acta, 11 (1975) 287.
77 Z. Gabelica, R. Hubin and E.G. Derovane, Thermochim. Acta, 24 (1978) 315.
78 M.J. Schmelz, T. Miyezawa, S. Mizushima, T.J. Lane and J.V. Quaglino, Spectrochim. Acta, 9 (1957) 51.
79 F. Douville, C. Duval and J. Lecompte, C.R. Acad. Sci., Ser. C, 212 (1941) 697.
80 F. Douville, C. Duval and J. Lecompte, Bull. Soc. Chim. Fr., 9 (1942) 548.
81 J.N. Vannikerk and F.R. Schoening, Acta Crystallogr., 4 (1951) 35.
82 K. Nakamoto, J. Fujita, S. Tanaka and M. Kobayashi, J. Am. Chem. Soc., 79 (1957) 4908.
83 J. Fujita, A.E. Martell and K. Nakamoto, J. Chem. Phys., 36 (1962) 324, 331.
84 E.C. Gruen and R.A. Plane, Inorg. Chem., 6 (1967) 1123.
85 M.P. Mathieau and H. Poulet, J. Chem. Phys., 59 (1962) 369.
86 S.P. Sinha, Spectrochim. Acta, 22 (1966) 57.
87 M. Jaber, F. Bertin and G. Thomas-David, Can. J. Chem., 56 (1978) 777.
88 V. Lorenzelli, G. Chauvet and B. Taravel, J. Mol. Struct., 45 (1985) 217.
89 W.O. DeConinck, Am. Chim. Anal., 22 (1917) 23.
90 D. Dollimore, G.R. Heal and N.P. Passalis, Thermochim. Acta, 92 (1985) 543.
91 A.S. Bhatti, D. Dollimore and A. Fletcher, Thermochim. Acta, 78 (1984) 63.
92 L. Watter-Levy and J. Laniepce, C.R. Acad. Sci., Ser. C, 258 (1964) 2038.
93 J.C. Mutin and G. Watelle-Marion, C.R. Acad. Sci., Ser. C, 266 (1968) 315.
94 D. Broadbent, D. Dollimore and J. Dollimore, Analyst (London), 94 (1969) 543.

95 P.K. Gallagher and C.R. Kurkjian, Inorg. Chem., 5 (1966) 214.
96 P.K. Gallagher, Inorg. Chem., 4 (1965) 965.
97 D. Broadbent, D. Dollimore and J. Dollimore, in R.F. Schwerker, Jr and P.D. Garn (Eds.), Thermal Analysis, Vol. 2, Academic Press, New York, 1969, p. 739.
98 T.B. Shkodina, E.I. Krylov and V.A. Sharov, Zh. Neorg. Khim., 17 (1972) 1823.
99 V.A. Sharov, E.A. Nikonenko, V.A. Pepelyaev, B.V. Zhadanov and E.I. Krylov, Koord. Khim., 4 (1978) 97.
100 T.M. Zhdanovshikh, E.I. Krylov, and V.A. Sharov, Zh. Neorg. Khim., 19 (1974), 2730.
101 W.W. Wendlandt, T.D. George and K.V. Khrishnamurthy, J. Inorg. Nucl. Chem., 21 (1961) 69.
102 N. Tanaka and M. Nanjo, Bull. Chem. Soc., Jpn., 40 (1967) 330.
103 K. Negase, Bull. Chem. Soc., Jpn., 45 (1972) 2166.
104 K. Negase, Bull. Chem. Soc., Jpn., 46 (1973) 144.
105 K. Negase, K. Sato and N. Tanaka, Bull. Chem. Soc., Jpn., 48 (1975) 868.
106 D. Mehandjiev, E. Zhecheva and S. Angelov, Thermochim. Acta, 95 (1985) 155.